$CsPb(Br/I)_3$ Perovskite Nanocrystals for Hybrid GaN-based High Bandwidth White Light-Emitting Diodes

Zhanhong Ma [1,2], Xiaodong Li [1], Chengxi Zhang [3,6] Lyudmila Turyanska [5], Shan Lin [1], Xin Xi [1], Jing Li [1], Tiangui Hu [1], Junfei Wang [1], Amalia Patanè [3] and Lixia Zhao [1,4]*

1 State Key Laboratory of Integrated Optoelectronics, Institute of Semiconductors, Chinese Academy of Sciences, Beijing 100083, China

2 School of Physics and Electronic-Electrical Engineering, Ningxia University, Yinchuan 750021, China

3 School of Physics and Astronomy, University of Nottingham, Nottingham NG7 2RD, UK

4 College of Electrical Engineering and Automation, Tiangong University, Tianjin 300387, China

5 Faculty of Engineering, University of Nottingham, Nottingham NG7 2RD, UK

6 Key Laboratory of Advanced Display and System Applications of Ministry of Education, Shanghai University, Shanghai 200072, China

Corresponding author: lxzhao@semi.ac.cn

Abstract

The modulation bandwidth of white light emitting diodes (LEDs) is an important factor in visible light communication (VLC) system, which is mainly limited by the down-conversion materials. The broad spectrum and long lifetime of conventional light conversion materials represent an obstacle to future technological developments. Here, we show that inorganic semiconductor perovskite nanocrystals offer a promising alternative nanomaterial. Anion exchange between different perovskite nanocrystals by post-synthesis is a highly efficient protocol to tune the chemical composition and optoelectronic properties of lead halide perovskite nanocrystals. The fine-tuning of the nanocrystal fluorescence is achieved by

blending colloidal solutions of $CsPb(Br/I)_3$ lead halide perovskites with different content of halide. The tunable optical emission and short fluorescence lifetime (< 5 ns) of the nanocrystals are exploited to realize white LEDs with a high modulation bandwidth (0.7 GHz), offering a potential route towards fast, energy efficient visible light communication.

KEYWORDS: perovskite, fluorescence lifetime, modulation bandwidth, anion exchange, visible light communication

1. Introduction

Amongst semiconductor technologies, III-nitride light emitting diodes (LEDs) have been significantly improved in recent years, resulting not only in the lighting revolution, but also stimulating new and innovative applications, such as visible light communication (VLC), an emerging technology to address the increasing bandwidth congestion for data communication. For VLC, LEDs can be modulated on and off at a high rate that is imperceptible to the human eye. Thus, functions of communication and lighting can be performed simultaneously.[1, 2] Compared with radio frequency wireless communications, VLC is more secure and is not limited by electromagnetic interference or license restrictions.[3, 4] White light sources for lighting and communication are commonly realized by combining a GaN-based blue LED and yellow phosphors.[5] However, the overall bandwidth of these white LEDs is only a few MHz, which severely restricts the data communication capacity of VLC systems.[6] This low bandwidth arises from the slow optical response of conventional cerium doped phosphors.[7-9] Furthermore, tuning the color rendering of these white LEDs is also challenging due to the limited tunability of the spectral properties of phosphors.

Semiconductor lead halide perovskite (LHP) nanocrystals (NCs) offer a promising alternative material system due to their tunable fluorescence emission by composition and/or quantum confinement. The LHPs have a ternary crystal structure $APbX_3$, where A is the cation site (A = Cs, CH_3NH_3 etc) and X is the halide site (X = Cl, Br, and I or mixed).[10, 11] In recent years all-inorganic perovskites containing a metal cation, such as cesium (Cs^+) have attracted significant attention due to high optical quantum yields and enhanced environmental stability,[12-16] compared to organic-based perovskites. All-inorganic NCs have been

successfully demonstrated in optoelectronic devices. For example, the external quantum efficiency (EQE) of perovskite LEDs (PeLEDs) based on green-emitting NCs can reach values of up to 24.5%, [17] offering potential applications in optoelectronics,[18] including lasers[19] and screen displays.[20, 21]

For applications that require tunable visible light sources, LHP NCs with different compositions have been used, e.g. blue and red fluorescence can be achieved in $CsPbCl_3$ and $CsPbI_3$ NCs, respectively.[14, 15] Mixing and/or changing the composition of the halide ion has pronounced effects on structural and optical properties of the NCs.[22] The diffusion and migration of halide ions in the perovskite lattice is known to result in the ion replacement; while thin films can be realized with halogen gases as sources to incorporate halide ions.[15, 23, 24] Also, the controlled substitution of the cations (*e.g.* Sn instead of Pb) can be used to tune the average NC size and optical properties.[25] This versatility offered by all-inorganic perovskite NCs is pivotal to the development of high quality light sources. Furthermore, the fluorescence lifetime of perovskites NCs is only of a few nanoseconds, which is an essential property required for applications of high-speed color converted materials in fast VLC.[12, 26]

In this study, we realize inorganic LHP NCs with tunable optical spectrum by blending as-synthesized green- and red-emitting colloidal $CsPbX_3$ (X = Br, I or mixture) NCs in solution. The controlled ion exchange and homogenization of the NC composition results in high quality $CsPb(Br:I)_3$ NCs, which not only have a fast recombination time (~ 5 ns) but a narrow spectral emission centered at wavelengths between those of the parent nanoparticles. Compared the synthetic methods of $CsPb(Br_xI_{1-x})_3$ reported previously,[24, 27] the post-synthesis via anion exchange process follows the Vegard's law, offering more flexibilities in controlling material compositions and properties beyond direct synthetic methodology. Therefore, this post-synthesis method of perovskite nanocrystals would be a good supplement to the existing synthetic methods. We select the composition of the NCs with quantum yield 45% to design and realize white LEDs that combine a blue InGaN-based micro-LED with a $CsPb(Br:I)_3$ NC film.[28] We demonstrate white LEDs with a modulation bandwidth of 0.7 GHz, which is higher than that achieved with conventional yellow phosphors about orders of magnitude.[6, 29] Thus, this route could offer opportunities for VLC that requires high-performance light sources for secure, fast and energy efficient wireless data transmission. In addition, previous reports for

blue LED+LHPs study paid little attention to the material characterization and analysis for the light converter. Here, the preparation of perovskite materials and post-synthesis process have been introduced systematically. During the post-synthesis, we found that the dependence of the PL peak energy on the Br content of $CsPb(Br/I)_3$ nanocrystals follows the Vegard's law. This is the first time to apply Vegard's law in perovskite material system. Furthermore, the optical properties of the LHPs have also been discussed. We believe these parts could help readers further understand the perovskites properties for VLC application.

2. Experimental section

2.1 Preparation of the Cs-precursor solution (Cs-oleate). Cs-oleate was synthesized as following method. Briefly, Cs_2CO_3 (1 mmol), 9 mL 1-octadecene (ODE) and 1.3 mL oleic acid (OA) were added in a 25 mL flask and degassed at 120 °C for 10 min under N_2 flow. Then, the temperature increased to 150 °C, and the mixture was stirred for 20 min under nitrogen flow. The Cs-oleate precursor kept 150 °C before use.

2.2 $CsPbX_3$ (X = Br, I) NCs synthesis. All-inorganic cesium lead halide perovskite NCs were synthesized as previously described.[10, 30] Typically, 20 mL of ODE, 2 mmol of PbI_2, 3 mL of OA and 3 mL of oleylamine (OLA) added in a 50 mL flask and degassed at 120 °C for 10 min under N_2 flow. Then the mixture was stirred at 150 °C for 20 min under nitrogen flow. A clear yellow solution of PbI_2-OA-OLA precursor was formed. The mixture was heated to 160 °C and 2 mL of Cs-oleate precursor was quickly injected. After 20 s mixing, the solution was cooled down to room temperature. For the $CsPb(Br_{0.4}I_{0.6})_3$ synthesis, 2 mmol of PbX_2 (the molar ratio of PbI_2 to $PbBr_2$ =2 : 3) were used to form $Pb(Br/I)_2$-OA-OLA precursor. For purification, 2.5 mL of the original solution was centrifuged at 2500 rpm for 5 min. The supernatant was further centrifuged at 12000 rpm for 10 min. The precipitate was collected and dissolved in 3 mL of a mixture of n-hexane and ethyl-acetate (1:3 v/v) and centrifuged at 12000 rpm for 10 min. Finally, the precipitate was collected and dispersed in n-hexane (5 mL) for storage in a fridge at T = 5°C. The structure, composition and synthesis processes of perovskite nanocrystals are shown in Scheme 1. To enhance the environmental stability and shelf life of the NCs, we used post synthesis ligand replacements with iminodiacetic acid

(IDA), following the method reported previously[31].

Scheme 1. Schematic Illustrations for the Structure/Composition and Synthesis Processes of Perovskite Nanocrystals.

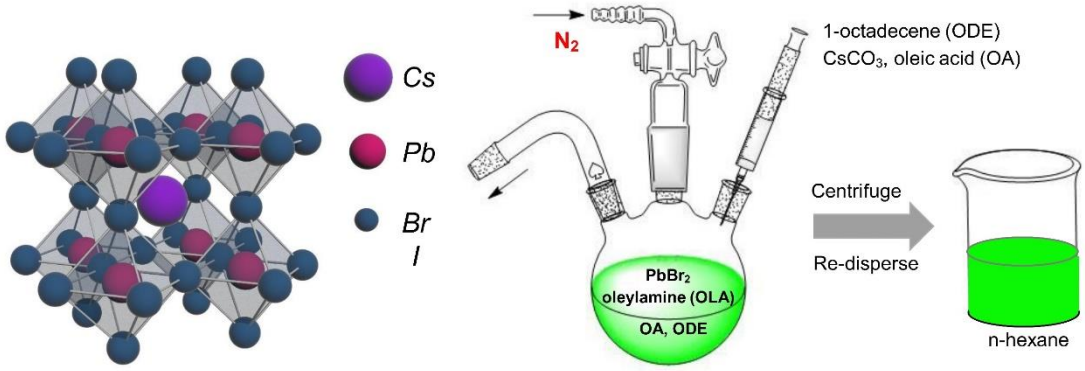

2.3 Post-synthesis $CsPb(Br:I)_3$ NCs preparation and measurements. $CsPb(Br:I)_3$ NCs with different composition were prepared by mixing NC solutions based on green $CsPbBr_3$ and red $CsPb(Br_{0.4}I_{0.6})_3$ NCs at a given molar ratio of Br in the two solutions, then ultrasonicated (~ 10 min) and mixed (~ 2 h) using a benchtop shaker. All processes were carried out in a glove box to avoid exposure of the NCs to oxygen and moisture. Samples were stored overnight in the glove box before characterization. For X-ray photoelectron spectroscopy (XPS) studies, the NC solution was drop-cast onto a gold/mica substrate. The XPS measurements were performed using a SPECS Phoibos 150 hemispherical analyzer and monochromatic Al-kα (1486.7 eV) X-ray source (pressure $P=1x10^{-9}$ mbar). Photoluminescence (PL) and time resolved PL (TRPL) spectra of the NCs were measured using an Edinburgh Instruments FLS980 fluorescence spectrometer equipped with a 375 nm laser diode as the excitation source. The optical absorption spectra were measured using a UV–vis near-infrared spectrophotometer (Varian Cary-5000).

2.4 InGaN-based blue micro-LED fabrication. An InGaN-based LED heterostructure was grown on a c-axial sapphire (0001) substrate by metal organic chemical vapor deposition (MOCVD).[4, 32] The details of epitaxial structure of the blue micro-LED chip shown in Fig. S6, Supporting Information.

After the epitaxial growth, the heterostructure was processed by standard micro-fabrication techniques into micro-LEDs with diameter of 30 μm. Firstly, the epitaxial wafer needs to be cleaned by using 3:1 volume ratio of sulfuric acid and hydrogen peroxide

mixed solution. Then the mesa pattern with diameter of 30μm was photolithographed and etched by using inductively coupled plasma (ICP). Afterwards, indium tin oxide film (ITO) was evaporated on the p-GaN surface using electron beam evaporation (EB), followed by the Cr/Al/Ti/Au deposition as ohmic contact electrodes. To protect and isolate the LED from the water and oxygen in the environment, the silicon dioxide protective layer was evaporated by plasma-enhanced chemical vapor deposition (PECVD), and the sapphire substrate needs to be thinned and polished within 150μm to improve the heat dissipation performance of micro-LED devices.

2.5 LED modulation bandwidth measurement system. The measurement system is comprised of Agilent E5061B vector network analyzer (VNA), bias-tee, DC power supply, photodetector (PD) and condenser lens. The test frequency range of VNA is 5 Hz ~ 3 GHz. The mode of VNA applied is S21 parameter (the ratio of output power to input power). The photodetector (PD) is silicon PIN detector from Newport Corporation (818-BB-21A), the 3dB bandwidth of the PD is from DC to 1.2 GHz. The details can be referred in our previous publications[33, 34].

3. Results and discussion

Our perovskite $CsPbX_3$ (X = Br, I or mixture) NCs are capped with a mixture of OA/OLA/IDA and have average diameter d = (14 ± 2) nm, as measured by transmission electron microscopy (Supporting Information, Figure S1). The room temperature (T = 300K) PL emission is centered at λ = 510 nm for green $CsPbBr_3$ NCs and at λ = 630 nm for red $CsPb(Br_{0.4}I_{0.6})_3$ NCs (Figure 1a). Mixing the two NC solutions results in yellow NCs with a PL emission centered at λ = 560 nm. The inset of Figure 1a shows the digital photographs of the corresponding green, red and yellow NCs dispersed in hexane under optical illumination.

To understand the origin of the PL shift of the mixture, we measured the PL spectra and UV-visible absorption spectra of the mixture of the $CsPbBr_3$ and $CsPb(Br_{0.4}I_{0.6})_3$ NCs in solution (Supporting Information, Figure S2). The PL peak position shifts from 2.43 eV (λ = 510 nm) for $CsPbBr_3$ to 2.05 eV (605 nm) following the addition of $CsPb(Br_{0.4}I_{0.6})_3$ NCs. We note that no PL peak corresponding to the original parent samples used to prepare the mixture

is observed. The dependence of the PL peak energy on the Br content is comparable to the reported emission energy for mixed halide perovskite NCs,[35] which follows the simple Vegard's law (Figure 1b). This suggests that the PL peak of the mixture is made of $CsPb(Br_xI_{1-x})_3$ NCs with a Br-content, *x*, intermediate between that of the original solutions. The UV-visible absorption spectra of the mixed solutions reveal that the absorption edge shifts to shorter wavelengths with increasing *x* (Supporting Information, Figure S2d). In addition, the full width half maxima (FWHM) of the PL emission of the mixture increases from 0.09 eV to 0.11eV, which we assign to the non-uniform composition distribution of the NCs in the solution, as observed in $CsPb(Br_xI_{1-x})_3$ NCs synthesized directly with different halide mixtures.[36]

Our results suggest that the chemical composition and optical properties of $CsPbX_3$ NCs can be tuned by post-synthesis mixing of $CsPbX_3$ (X = Br, I) NC solutions with different halogen content due to an anion exchange process involving different NCs (inset of Figure 1b). The XPS studies were performed to assess the change of composition of the NCs (Supporting Information, Figure S3).

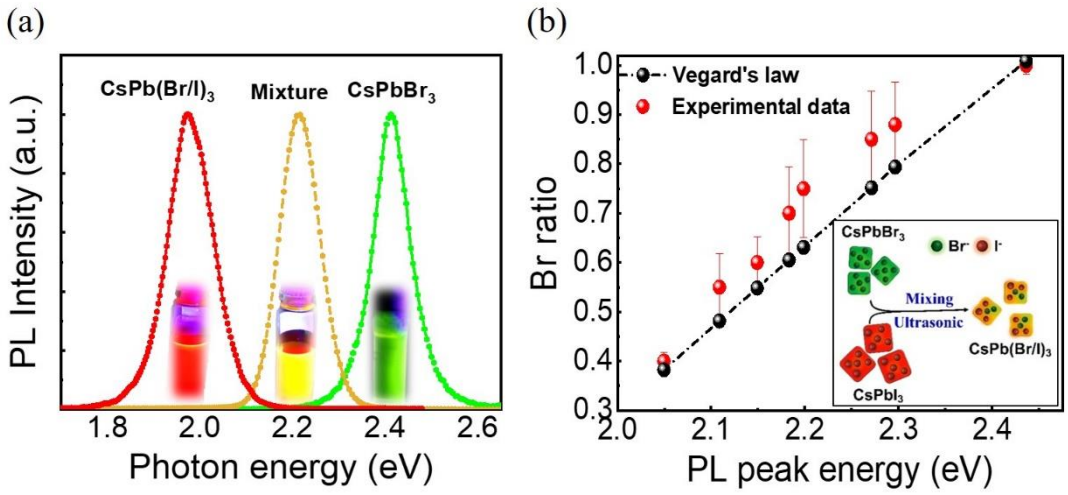

Figure 1 (a) Room temperature normalized photoluminescence spectra of $CsPbBr_3$ (green), $CsPb(Br/I)_3$ Br:I=2:3 (red), and the mixture of green and red perovskite NCs dispersed in hexane with similar NC concentration. Inset: digital photograph of the NCs dispersed in hexane under 365nm illumination. (b) Dependence of the PL peak energy on the molar ratio of Br/I in the $CsPb(Br/I)_3$ NCs. Inset: Schematic diagram of the anion exchange process, which takes place in mixed solution of green and red NCs.

Figure 2a shows the PL spectrum and fluorescence lifetime of the mixed NCs under

excitation with a 375 nm laser. In this experiment, two samples were considered: a NC solution and a film obtained by spin-coating the NCs on a transparent quartz substrate. The fluorescence lifetimes of the NC film (τ ~5 ns at wavelengths corresponding to the PL peak) is one order of magnitude shorter compared to that of the NC solution (τ ~22 ns). To further understand the trap state, the PL lifetimes were calculated by fitting the PL decay curves using the bi-exponential decay function, as shown in Table S1 (Supporting Information). The fast radiation lifetime τ1 decreases from 7.42 ns to 3.04 ns, almost half of the value for perovskite nanocrystal solution. In general, the fast-lifetime component is related to the surface defect state, and the slow-lifetime component is due to the electron-hole pair recombination process. Therefore, the trap-state related recombination is more remarkable in the NC film.[37] An increase of PL lifetime with increasing wavelength across the PL line is observed for both NCs in the film and in solution. This is because the excited light 375 nm would induce the electron transition from valence band (VB) to high energy levels of conduction band (CB). Some high energy-level electrons direct recombine with holes in the VB and emit photon with shorter wavelength with a short recombination lifetime. Besides, part of electrons would have relaxation from the high energy levels of the CB to the low energy levels, and then have the radiative recombination with the valence-band holes, resulting in a longer wavelength emission. The recombination lifetime is also longer compared with the direct recombination of higher energy-level electron-hole pairs.[38]

To investigate further the difference in PL lifetime for the NC solutions and films, we studied the influence of the perovskite concentration and excitation power on the fluorescence lifetime, the TRPL studies were performed. We found that for solution with NC concentration ranging from 0.025 mg/mL to 0.15 mg/mL, the NC concentration does not significantly affect the fluorescence lifetime (Figure 2b and Figure S4, Supporting information). In addition, the TRPL spectra were recorded for the NCs in film (Figure 2c) and in solution (Figure S5, Supporting information) under different laser powers. The results show that the fluorescence lifetime of the NC solution (0.05 mg/mL) is independent of the laser power, but the excitation power can affect the fluorescence lifetime for the NC film, as shown in Fig. 2d. The lifetime decreases from τ = 9.2 to 5.5 ns with increasing the laser power from 0.15 to 2.4 μW, which are the laser emission power. The 375 nm pulsed laser was used in the TRPL spectra

measurement. The laser powers here are the emission light power in the position of test samples collected by an optical power meter. The difference between the solution and film indicates the existence of an additional exciton relaxation channel for the NCs in the film, which is power-dependent. The difference between the perovskite nanocrystal solution and film is that the nanocrystals are separated from each other in solution, but stick to each other in NC film. Therefore, the charge transfer is easier to occur between nanocrystals in NC film, which is accompanied by nonradiative energy transfer. When the excitation power increases, many electrons transition and transfer to adjacent nanocrystals, promoting the nonradiative energy transfer and resulting the decrease of radiative lifetime of the perovskite nanocrystals.[39, 40] The fluorescence lifetime of the perovskite NC film is one order of magnitude shorter than that of the commercial phosphors, such as Yttrium aluminum garnet (YAG),[9, 41] confirming its potential as optical conversion material for white LEDs.

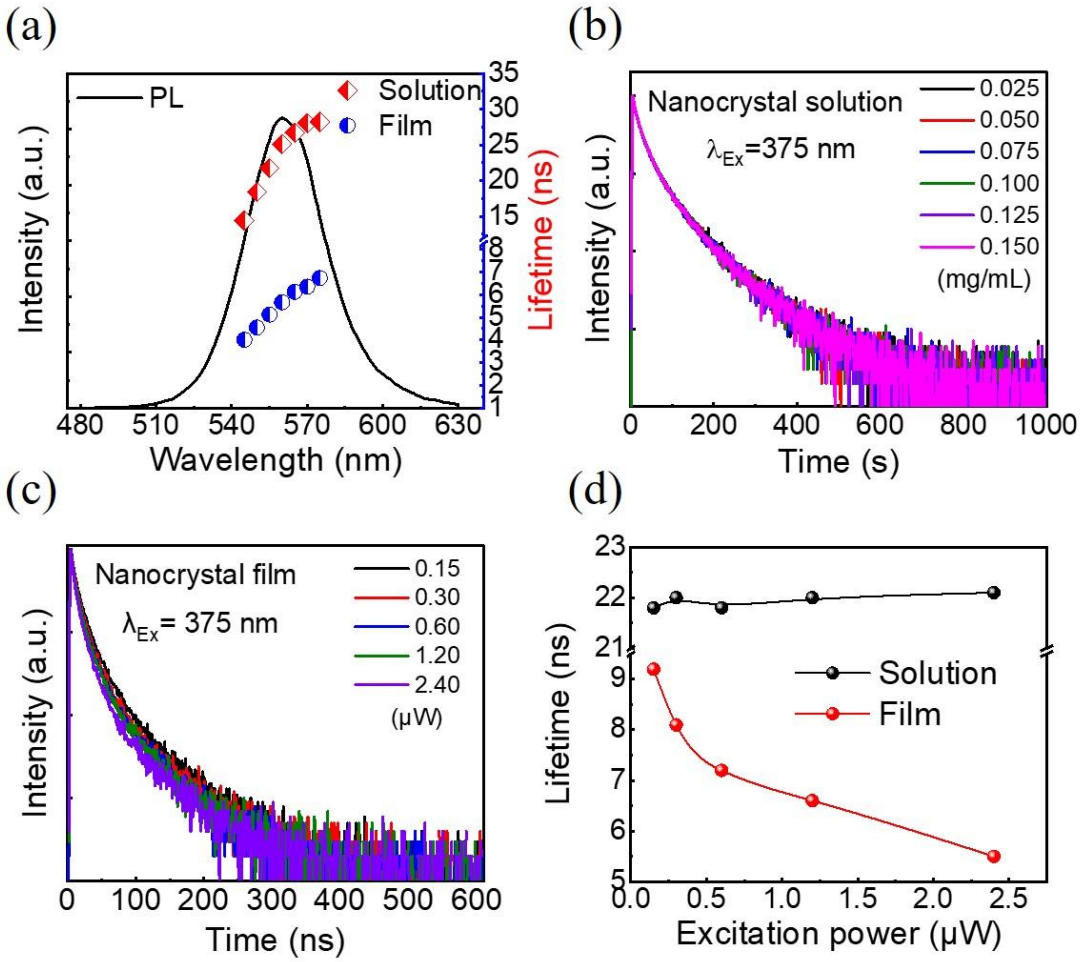

Figure 2 (a) The PL spectrum of the perovskite NC mixture and the fluorescence lifetime as a function of

the emission wavelength for a NC solution and a NC film. (b) TRPL spectra for solutions with different concentrations of NCs. (c) TRPL spectra of a NC film under different laser excitation powers (λ = 375 nm). (d) The fluorescence lifetimes of the NC solution (0.05mg/mL) and film as derived from the analysis of the TRPL spectra.

The tunability and the short-lifetime make the perovskite NCs great potential for fabricating white LEDs. Figure 3a shows the schematic diagram and optical image of the white LED, which is based on a blue InGaN-LED coated with a layer of NCs. Following the fabrication of an LED chip with diameter d = 30 μm, a solution of the mixed NCs in hexane was spin coated on the surface of the LED in a glove box. Then, the device was left in the glove box overnight to fully evaporate the solvent (hexane). To avoid contamination and degradation of the perovskite NC film in air, and hence to achieve optimal light extraction, the device was coated using a protective layer of UV glue, which possesses high optical transparency, chemical inertness, and high-temperature stability.[28, 31]

Two white LEDs were fabricated using mixtures of the NCs with different ratio of Br/I. The emission of the fabricated LEDs can be fine tuned by the composition of the perovskite NC layer. Figure 3b shows the calculated chromatic coordinates of the hybrid LEDs plotted in the CIE 1931 color space. When the ratio of Br in the green to red perovskites is G: R=1:2 (e.g. Br-content x = 0.65), the chromatic coordinates (x, y) of the hybrid LED changes from (0.3107, 0.4557) to (0.2726, 0.3570) with increasing the current from I = 10 to 100 mA. The correlated color temperature (CCT) of the hybrid white LED with G: R=1:2 changes from 6078 to 7865 K with increasing the current from 10 to 100 mA. While the D_{uv}, the distance from the chromaticity coordinates of the source to the Planckian locus on the CIE chromaticity diagram,[42, 43] changes from 0.071 to 0.048. In addition, the luminous efficiency and luminous efficacy of the perovskite white LED have been compared with the conventional YAG-coated white LED (with the same blue micro-LED chip)，details can be inferred in the supporting information. If the ratio decreases to G: R=1:4 (x = 0.6), the chromatic coordinates (x, y) of the perovskite mixture changes from (0.3933, 0.4695) to (0.3326, 0.367) with increasing current from I = 10 to 100 mA. The CCT of the hybrid white LED with G: R=1:4 changes from 4229 to 5501 K with increasing the current from 10 to 100

mA, and the Duv for the white LED shifts from 0.047 to 0.019. This is within the white region of the CIE 1931 color space, as further illustrated by the optical photograph of the white LED in Fig. 3c. As we can see, the emitting wavelength of the NC light conversion layer can be tuned to adjust the color quality of the white LEDs. With the increase of the proportion of iodine component in $CsPb(Br_xI_{1-x})_3$ nanocrystals, the CCT of white LED gradually decreases, the light color changes from cold white light to warm white light. The cold white light source can serve as the headlight of vehicle, realizing the lighting and communication in the traffic simultaneously. While the warm light source shows great potential for the indoor application to offer dual function of the lighting and communication. Therefore, due to the highly saturated colors and the intrinsic tunability nature of the perovskite NCs, the color quality of white LEDs can be improved significantly.[18, 44]

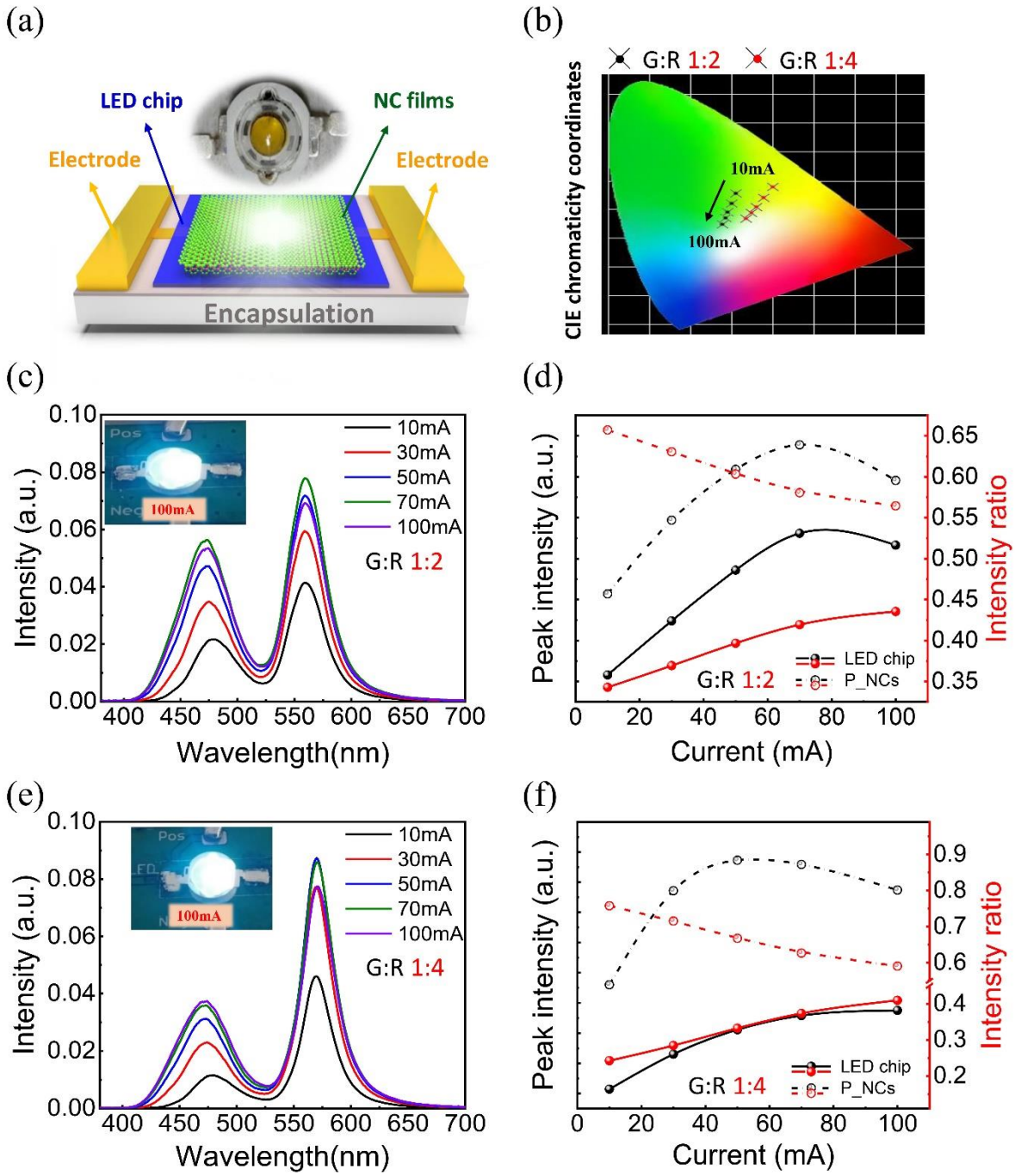

Figure 3 (a) Schematic diagram and optical image of the white LED device using the mixture perovskite NCs s and a GaN-based blue LED chip. (b) The calculated chromaticity coordinates of the hybrid LED plotted using a CIE 1931 color space. (c) Room temperature (T = 300 K) luminescence spectra for hybrid III-Nitride/inorganic $CsPbX_3$ perovskite NC white LEDs under different injection currents for a molar ratio of green and red NCs of 1:2. (d) Dependence of the intensity of the NC (red) and LED chip (black) emission on the injection current for a molar ratio of green and red NCs of 1:2. The solid line corresponds to the LED chip and the dotted line to the perovskite NCs (P_NCs). (e) Room temperature (T = 300 K)

luminescence spectra for hybrid III-Nitride/inorganic $CsPbX_3$ perovskite NC white LEDs under different injection currents for a molar ratio of green and red NC of 1:4(f) Dependence of the intensity of the NC (red) and LED chip (black) emission on the injection current for a molar ratio of green and red nanocrystals of 1:4. The solid line is for the LED chip and the dotted line is for the NCs.

Figure 3c shows the dependence of the luminescence of the hybrid LED with a mole ratio of green and red NCs G: R=1:2 (x = 0.65). The electroluminescence (EL) emission of the InGaN/GaN MQWs is centered at 470 nm and the emission from the NC films is centered at 560 nm, which is consistent with the PL peak wavelength of the mixed NC solution (Figure 1a and 2a). When the injection current is below 70 mA, the EL intensity from the MQWs and the luminescence intensity of the NC film increase with increasing the injection current *I*, as shown in Fig. 3d. However, as the current increases further, there is a drop of light emission intensity when the current up to 80 mA.

In addition, the EL intensity integral ratio of LED chip is defined as $R_{LED-chip} = \int EL_{LED-chip} \Big/ \oint EL$, the EL intensity integral ratio of NC film in hybrid LED is defined as $R_{NC-film} = \int EL_{NC-film} \Big/ \oint EL$. The EL intensity integral ratios of LED chip and NC film from the EL spectra show that the intensity ratio of the LED chip increases monotonically with increasing the current, but the intensity ratio for NC films decreases monotonically with the current increase. This behavior may be related to the heating effect. To further verify this view, the junction temperature (Tj) of the micro-LED and the PL stability of the nanocrystal (NC) film were measured (Supporting Information, Fig. S7a and S7b). The Tj at 10 mA is close to room temperature, but when the injection current increases to 100 mA, the Tj is up to 64℃. The PL intensity of the NC film decreases with the temperature increasing. Furthermore, dangling bonds can be generated at high temperatures,[31, 45] which act as trap states for carriers, resulting in an irreversible quenching of the NC luminescence (Supporting Information, Figure S7c).

Figure 3e shows the current dependent spectra of the hybrid white LEDs with a mole ratio of green and red nanocrystals of G: R=1:4. Compared to the LEDs with G: R=1:2 in Fig. 3c, the saturation point of the NC intensity with increasing the current occurs at a lower current (*I*

= 50 mA, as shown in Fig. 3f). The peak intensity of the NC film with ratio G: R=1:4 is larger than that of G: R=1:2. In addition, the peak intensity of the white LED with G: R=1:4 is lower than that of G: R=1:2, suggesting that the perovskite NCs with more iodine ions in the mixture can absorb more blue light from the LED chip (Figure S2d, Supporting Information).

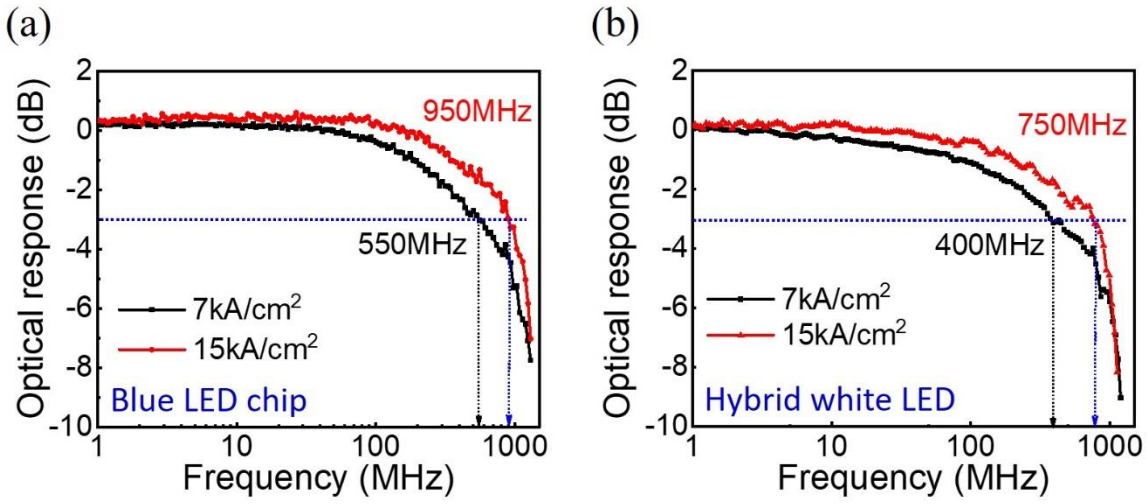

Figure 4 Frequency response of the blue micro-LED chip (a) and the hybrid white LED device (b) at different current densities (7kA/cm^2, 15kA/cm^2).

The frequency response of the blue micro-LED chip and the hybrid white LEDs were measured from 100 kHz to 1.2 GHz using a network analyzer. Figure 4a shows the frequency response for the blue micro-LED chip: at 7 kA/cm^2 and 15 kA/cm^2, the modulation bandwidth f_{-3dB} is 550 MHz and 950 MHz, respectively. When using the mixed perovskite NC film as the optical converted material of the hybrid white LED, the f_{-3dB} of the white LED under 7 kA/cm^2 and 15 kA/cm^2 is 400 MHz and 750 MHz, as shown in Fig. 4b. Using the frequency response functions of the blue LED chip and light conversion material,[26, 28] the theoretical 3dB modulation bandwidth of the $CsPb(Br/I)_3$ perovskite nanocrystals for hybrid GaN-based white LED can be calculated to be 350 MHz at 7 kA/cm^3, 710 MHz at 15 kA/cm^3, which coincides with the experimental measurement. These high modulation bandwidths are due to the short fluorescence lifetime of the perovskite NC film, much shorter than that of CdSe/ZnS quantum dots or YAG phosphors. This property combined with the high modulation bandwidth of the blue micro-LED chip enable us to achieve the highest modulation bandwidth for light-converted white LEDs.[28, 46] Thus, these results indicate that

perovskite-based light sources with all inorganic lead-halide-based perovskites NC films have potential to overcome the limitation of current white light sources for future light communication. With further improvement of the fluorescence conversion efficiency of perovskite nanocrystals as well as the optical power of GaN-based LED chip, the bandwidth of hybrid GaN-based white LED can be further enhanced.

4. Conclusion

In this study, we prepared different inorganic lead-halide-based perovskites NCs. Results show that by post-synthesis treatments and blending green and red colloidal $CsPbX_3$ (X = Br, I) NCs in solution, the chemical composition and optical properties of $CsPbX_3$ NCs can be tuned due to an anion (Br, I) exchange dynamic process. This approach enables us to produce homogenous mixtures of perovskite NCs emitting in a narrow spectral region. The fluorescence lifetime measurements show that after spin-coating the NC solution on a transparent quartz substrate, the lifetime of the NC film decreases. This decreases further with increasing the excitation power or for NCs emitting at shorter wavelengths. By the design of the appropriate spectral region of the mixed $CsPb(Br/I)_3$ NCs (emission wavelength 560-570 nm) and short fluorescence lifetime of the NC film, a novel type of hybrid white LED with a high modulation bandwidth was fabricated. This combines colloidal nanocrystals with a well-established III–V semiconductor micro-LED and can be further developed for VLC, an emerging technology that requires high-performance visible light sources for secure, fast energy-efficient wireless transmission.

Supporting Information

SI1. TEM image of perovskite nanocrystals; SI2. PL properties of perovskite solutions; SI3. XPS studies; SI4. TRPL studies of perovskite nanocrystal solution and film; SI5. TRPL spectra of perovskite NC solution with different concentrations; SI6. TRPL spectra of NC solution under different excitation powers; SI7. Epitaxial structure of the blue LED chip; SI8. Stability of white LEDs.

Author Information

Corresponding Author:

Lixia Zhao - State Key Laboratory of Integrated Optoelectronics, Institute of Semiconductors, Chinese Academy of Sciences, Beijing 100083, China; College of Electrical Engineering and Automation, Tiangong University, Tianjin 300387, China; Email: lxzhao@semi.ac.cn; orcid.org/0000-0002-0466-247X.

Authors:

Zhanhong Ma - School of Physics and Electronic-Electrical Engineering, Ningxia University, Yinchuan 750021, China; State Key Laboratory of Integrated Optoelectronics, Institute of Semiconductors, Chinese Academy of Sciences, Beijing 100083, China; Email: mzh@nxu.edu.cn; orcid.org/0000-0003-1029-3882.

Xiaodong Li - State Key Laboratory of Integrated Optoelectronics, Institute of Semiconductors, Chinese Academy of Sciences, Beijing 100083, China; Email: xdli@semi.ac.cn.

Chengxi Zhang - School of Physics and Astronomy, University of Nottingham, Nottingham NG7 2RD, UK; Key Laboratory of Advanced Display and System Applications of Ministry of Education, Shanghai University, Shanghai 200072, China; Email: xi1273424183@163.com.

Lyudmila Turyanska - Faculty of Engineering, University of Nottingham, Nottingham NG7 2RD, UK; Email: lyudmila.turyanska@nottingham.ac.uk; orcid.org/0000-0002-9552-6501.

Shan Lin - State Key Laboratory of Integrated Optoelectronics, Institute of Semiconductors, Chinese Academy of Sciences, Beijing 100083, China; Email: linshan@semi.ac.cn.

Xin Xi - State Key Laboratory of Integrated Optoelectronics, Institute of Semiconductors, Chinese Academy of Sciences, Beijing 100083, China; Email: xixin@semi.ac.cn.

Jing Li - State Key Laboratory of Integrated Optoelectronics, Institute of Semiconductors, Chinese Academy of Sciences, Beijing 100083, China; Email: jingl@semi.ac.cn.

Tiangui Hu - State Key Laboratory of Integrated Optoelectronics, Institute of Semiconductors, Chinese Academy of Sciences, Beijing 100083, China; Email: tghu@semi.ac.cn.

Junfei Wang - State Key Laboratory of Integrated Optoelectronics, Institute of

Semiconductors, Chinese Academy of Sciences, Beijing 100083, China; Email: junfeiwang@semi.ac.cn.

Amalia Patanè - School of Physics and Astronomy, University of Nottingham, Nottingham NG7 2RD, UK; Email: amalia.patane@nottingham.ac.uk.

Acknowledgments

This work is funded by the National Natural Science Foundation of China (Grant Nos. 61774148, 11974343); the Engineering and Physical Sciences Research Council (Grant Nos. EP/K503800/1, NC/L001861/1).

References

1. Haas, H.; Yin, L.; Wang, Y.; Chen, C., What is LiFi? *Journal of Lightwave Technology* **2016,** *34* (6), 1533-1544.

2. Feezell, D.; Nakamura, S., Invention, development, and status of the blue light-emitting diode, the enabler of solid-state lighting. *Comptes Rendus Physique* **2018,** *19* (3), 113-133.

3. Zhao, L.; Zhu, S.; Wu, C.; Yang, C.; Yu, Z.; Yang, H.; Liu, L., GaN-based LEDs for light communication. *Science China Physics, Mechanics & Astronomy* **2016,** *59* (10), 107301.

4. Zhu, S.; Lin, S.; Li, J.; Yu, Z.; Cao, H.; Yang, C.; Li, J.; Zhao, L., Influence of quantum confined Stark effect and carrier localization effect on modulation bandwidth for GaN-based LEDs. *Applied Physics Letters* **2017,** *111* (17), 171105.

5. Lin, C. C.; Liu, R. S., Advances in Phosphors for Light-emitting Diodes. *J Phys Chem Lett* **2011,** *2* (11), 1268-77.

6. Rajbhandari, S.; McKendry, J. J. D.; Herrnsdorf, J.; Chun, H.; Faulkner, G.; Haas, H.; Watson, I. M.; O'Brien, D.; Dawson, M. D., A review of gallium nitride LEDs for multi-gigabit-per-second visible light data communications. *Semiconductor Science and Technology* **2017,** *32* (2), 023001.

7. Li, H.; Zhang, Y.; Chen, X.; Wu, C.; Guo, J.; Gao, Z.; Pei, W.; Chen, H., 682Mbit/s phosphorescent white LED visible light communications utilizing analog equalized 16QAM-OFDM modulation without blue filter. *Optics Communications* **2015,** *354*, 107-111.

8. Yeh, C. H.; Liu, Y. L.; Chow, C. W., Real-time white-light phosphor-LED visible light communication (VLC) with compact size. *Optics express* **2013,** *21* (22), 26192-7.

9. Ma, Z.; Cao, H.; Sun, X.; Yang, C.; Xi, X.; Li, J.; Lin, S.; Zhao, L., Failure Mechanism of Phosphors in GaN‐Based White LEDs. *physica status solidi (a)* **2019,** *216* (6), 1800335.

10. Akkerman, Q. A.; Raino, G.; Kovalenko, M. V.; Manna, L., Genesis, challenges and opportunities for colloidal lead halide perovskite nanocrystals. *Nat Mater* **2018,** *17* (5), 394-405.

11. Chiba, T.; Kido, J., Lead halide perovskite quantum dots for light-emitting devices. *Journal of Materials Chemistry C* **2018,** *6* (44), 11868-11877.

12. Lu, M.; Zhang, X.; Bai, X.; Wu, H.; Shen, X.; Zhang, Y.; Zhang, W.; Zheng, W.; Song, H.; Yu, W. W.; Rogach, A. L., Spontaneous Silver Doping and Surface Passivation of CsPbI3 Perovskite Active Layer Enable Light-Emitting Devices with an External Quantum Efficiency of 11.2. *ACS Energy Lett* **2018,** *3* (7),

1571-1577.
13. Shi, Z.; Li, Y.; Zhang, Y.; Chen, Y.; Li, X.; Wu, D.; Xu, T.; Shan, C.; Du, G., High-Efficiency and Air-Stable Perovskite Quantum Dots Light-Emitting Diodes with an All-Inorganic Heterostructure. *Nano Lett* **2017,** *17* (1), 313-321.
14. Protesescu, L.; Yakunin, S.; Bodnarchuk, M. I.; Krieg, F.; Caputo, R.; Hendon, C. H.; Yang, R. X.; Walsh, A.; Kovalenko, M. V., Nanocrystals of Cesium Lead Halide Perovskites (CsPbX(3), X = Cl, Br, and I): Novel Optoelectronic Materials Showing Bright Emission with Wide Color Gamut. *Nano Lett* **2015,** *15* (6), 3692-6.
15. Nedelcu, G.; Protesescu, L.; Yakunin, S.; Bodnarchuk, M. I.; Grotevent, M. J.; Kovalenko, M. V., Fast Anion-Exchange in Highly Luminescent Nanocrystals of Cesium Lead Halide Perovskites (CsPbX3, X = Cl, Br, I). *Nano Lett* **2015,** *15* (8), 5635-40.
16. Huang, H.; Bodnarchuk, M. I.; Kershaw, S. V.; Kovalenko, M. V.; Rogach, A. L., Lead Halide Perovskite Nanocrystals in the Research Spotlight: Stability and Defect Tolerance. *ACS Energy Lett* **2017,** *2* (9), 2071-2083.
17. Shen, Y.; Li, M. N.; Li, Y.; Xie, F. M.; Wu, H. Y.; Zhang, G. H.; Chen, L.; Lee, S. T.; Tang, J. X., Rational Interface Engineering for Efficient Flexible Perovskite Light-Emitting Diodes. *ACS nano* **2020,** *14* (5), 6107-6116.
18. Kovalenko, M. V.; Protesescu, L.; Bodnarchuk, M. I., Properties and potential optoelectronic applications of lead halide perovskite nanocrystals. *Science* **2017,** *358* (6364), 745.
19. Yakunin, S.; Protesescu, L.; Krieg, F.; Bodnarchuk, M. I.; Nedelcu, G.; Humer, M.; De Luca, G.; Fiebig, M.; Heiss, W.; Kovalenko, M. V., Low-threshold amplified spontaneous emission and lasing from colloidal nanocrystals of caesium lead halide perovskites. *Nature communications* **2015,** *6*, 8056.
20. Shan, Q.; Song, J.; Zou, Y.; Li, J.; Xu, L.; Xue, J.; Dong, Y.; Han, B.; Chen, J.; Zeng, H., High Performance Metal Halide Perovskite Light-Emitting Diode: From Material Design to Device Optimization. *Small* **2017,** *13* (45), 1701770.
21. Veldhuis, S. A.; Boix, P. P.; Yantara, N.; Li, M.; Sum, T. C.; Mathews, N.; Mhaisalkar, S. G., Perovskite Materials for Light-Emitting Diodes and Lasers. *Adv Mater* **2016,** *28* (32), 6804-34.
22. D'Innocenzo, V.; Srimath Kandada, A. R.; De Bastiani, M.; Gandini, M.; Petrozza, A., Tuning the light emission properties by band gap engineering in hybrid lead halide perovskite. *J Am Chem Soc* **2014,** *136* (51), 17730-3.
23. Pellet, N.; Teuscher, J.; Maier, J.; Grätzel, M., Transforming Hybrid Organic Inorganic Perovskites by Rapid Halide Exchange. *Chemistry of Materials* **2015,** *27* (6), 2181-2188.
24. Lv, W.; Tang, X.; Li, L.; Xu, L.; Li, M.; Chen, R.; Huang, W., Assessment for Anion-Exchange Reaction in CsPbX3 (X = Cl, Br, I) Nanocrystals from Bond Strength of Inorganic Salt. *The Journal of Physical Chemistry C* **2019,** *123* (39), 24313-24320.
25. Hao, F.; Stoumpos, C. C.; Cao, D. H.; Chang, R. P. H.; Kanatzidis, M. G., Lead-free solid-state organic–inorganic halide perovskite solar cells. *Nature Photonics* **2014,** *8* (6), 489-494.
26. Xue, D.; Ruan, C.; Zhang, Y.; Chen, H.; Chen, X.; Wu, C.; Zheng, C.; Chen, H.; Yu, W. W., Enhanced bandwidth of white light communication using nanomaterial phosphors. *Nanotechnology* **2018,** *29* (45), 455708.
27. Chen, X.; Peng, L.; Huang, K.; Shi, Z.; Xie, R.; Yang, W., Non-injection gram-scale synthesis of cesium lead halide perovskite quantum dots with controllable size and composition. *Nano Research* **2016,** *9* (7), 1994-2006.
28. Cao, H.; Lin, S.; Ma, Z.; Li, X.; Li, J.; Zhao, L., Color Converted White Light-Emitting Diodes With 637.6 MHz Modulation Bandwidth. *IEEE Electron Device Letters* **2019,** *40* (2), 267-270.
29. Brien, D. C. O.; Zeng, L.; Le-Minh, H.; Faulkner, G.; Walewski, J. W.; Randel, S. In *Visible light*

communications: Challenges and possibilities, 2008 IEEE 19th International Symposium on Personal, Indoor and Mobile Radio Communications, 15-18 Sept. 2008; 2008; pp 1-5.

30. Wang, Y.; Li, X.; Song, J.; Xiao, L.; Zeng, H.; Sun, H., All-Inorganic Colloidal Perovskite Quantum Dots: A New Class of Lasing Materials with Favorable Characteristics. *Adv Mater* **2015,** *27* (44), 7101-8.

31. Zhang, C.; Turyanska, L.; Cao, H.; Zhao, L.; Fay, M. W.; Temperton, R.; O'Shea, J.; Thomas, N. R.; Wang, K.; Luan, W.; Patane, A., Hybrid light emitting diodes based on stable, high brightness all-inorganic CsPbI3 perovskite nanocrystals and InGaN. *Nanoscale* **2019**, 13450-13457.

32. Shan, L.; Haicheng, C.; Jing, L.; Xuejiao, S.; Huixin, X.; Lixia, Z., Modulation and optoelectronic properties of GaN-based light-emitting diodes on GaN template. *Applied Physics Express* **2018,** *11* (12), 122101.

33. Zhu, S. C.; Yu, Z. G.; Zhao, L. X.; Wang, J. X.; Li, J. M., Enhancement of the modulation bandwidth for GaN-based light-emitting diode by surface plasmons. *Optics express* **2015,** *23* (11), 13752-60.

34. Zhu, S.; Wang, J.; Yan, J.; Zhang, Y.; Pei, Y.; Si, Z.; Yang, H.; Zhao, L.; Liu, Z.; Li, J. J. E. S. S. L., Influence of AlGaN Electron Blocking Layer on Modulation Bandwidth of GaN-Based Light Emitting Diodes. **2014,** *3* (3), R11-R13.

35. Beal, R. E.; Slotcavage, D. J.; Leijtens, T.; Bowring, A. R.; Belisle, R. A.; Nguyen, W. H.; Burkhard, G. F.; Hoke, E. T.; McGehee, M. D., Cesium Lead Halide Perovskites with Improved Stability for Tandem Solar Cells. *J Phys Chem Lett* **2016,** *7* (5), 746-51.

36. Song, J.; Li, J.; Li, X.; Xu, L.; Dong, Y.; Zeng, H., Quantum Dot Light-Emitting Diodes Based on Inorganic Perovskite Cesium Lead Halides (CsPbX3). *Adv Mater* **2015,** *27* (44), 7162-7.

37. Zhang, Z. Y.; Wang, H. Y.; Zhang, Y. X.; Hao, Y. W.; Sun, C.; Zhang, Y.; Gao, B. R.; Chen, Q. D.; Sun, H. B., The Role of Trap-assisted Recombination in Luminescent Properties of Organometal Halide CH3NH3PbBr3 Perovskite Films and Quantum Dots. *Sci Rep* **2016,** *6*, 27286.

38. Mondal, N.; Samanta, A., Complete ultrafast charge carrier dynamics in photo-excited all-inorganic perovskite nanocrystals (CsPbX3). *Nanoscale* **2017,** *9* (5), 1878-1885.

39. Zhang, J.; Zhu, X.; Wang, M.; Hu, B., Establishing charge-transfer excitons in 2D perovskite heterostructures. *Nature communications* **2020,** *11* (1), 2618.

40. Luo, X.; Liang, G.; Han, Y.; Li, Y.; Ding, T.; He, S.; Liu, X.; Wu, K., Triplet Energy Transfer from Perovskite Nanocrystals Mediated by Electron Transfer. *J Am Chem Soc* **2020,** *142* (25), 11270-11278.

41. Wall, W. A.; Karpick, J. T.; Bartolo, B. D., Temperature dependence of the vibronic spectrum and fluorescence lifetime of YAG:Cr3+. *Journal of Physics C: Solid State Physics* **1971,** *4* (18), 3258-3264.

42. Zhu, P.; Zhu, H.; Adhikari, G. C.; Thapa, S., Design of circadian white light-emitting diodes with tunable color temperature and nearly perfect color rendition. *OSA Continuum* **2019,** *2* (8), 2413-2427.

43. Zhu, P.; Zhu, H.; Adhikari, G. C.; Thapa, S., Spectral optimization of white light from hybrid metal halide perovskites. *OSA Continuum* **2019,** *2* (6), 1880-1888.

44. Cortecchia, D.; Yin, J.; Petrozza, A.; Soci, C., White light emission in low-dimensional perovskites. *Journal of Materials Chemistry C* **2019,** *7* (17), 4956-4969.

45. An, R.; Zhang, F.; Zou, X.; Tang, Y.; Liang, M.; Oshchapovskyy, I.; Liu, Y.; Honarfar, A.; Zhong, Y.; Li, C.; Geng, H.; Chen, J.; Canton, S. E.; Pullerits, T.; Zheng, K., Photostability and Photodegradation Processes in Colloidal CsPbI3 Perovskite Quantum Dots. *ACS applied materials & interfaces* **2018,** *10* (45), 39222-39227.

46. Dursun, I.; Shen, C.; Parida, M. R.; Pan, J.; Sarmah, S. P.; Priante, D.; Alyami, N.; Liu, J.; Saidaminov, M. I.; Alias, M. S.; Abdelhady, A. L.; Ng, T. K.; Mohammed, O. F.; Ooi, B. S.; Bakr, O. M., Perovskite Nanocrystals as a Color Converter for Visible Light Communication. *ACS Photonics* **2016,** *3* (7), 1150-1156.

Table of Contents graphic